Accepted Manuscript

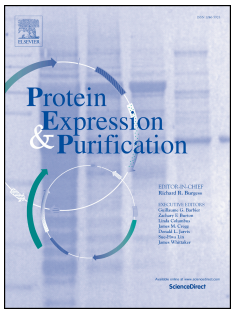

Method for rapid optimization of recombinant GPCR protein expression and stability using virus-like particles

Thao T. Ho, Jasmine T. Nguyen, Juping Liu, Pawel Stanczak, Aaron A. Thompson, Yingzhuo G. Yan, Jasmine Chen, Charles K. Allerston, Charles L. Dillard, Hao Xu, Nicholas J. Shoger, Jill S. Cameron, Mark E. Massari, Kathleen Aertgeerts

PII: S1046-5928(16)30483-1

DOI: 10.1016/j.pep.2017.03.002

Reference: YPREP 5061

To appear in: *Protein Expression and Purification*

Received Date: 21 December 2016

Revised Date: 24 February 2017

Accepted Date: 1 March 2017

Please cite this article as: T.T. Ho, J.T. Nguyen, J. Liu, P. Stanczak, A.A. Thompson, Y.G. Yan, J. Chen, C.K. Allerston, C.L. Dillard, H. Xu, N.J. Shoger, J.S. Cameron, M.E. Massari, K. Aertgeerts, Method for rapid optimization of recombinant GPCR protein expression and stability using virus-like particles, *Protein Expression and Purification* (2017), doi: 10.1016/j.pep.2017.03.002.

Method for Rapid Optimization of Recombinant GPCR Protein Expression and Stability using Virus-Like Particles

Thao T. Ho[1]*, Jasmine T. Nguyen[1]*, Juping Liu[2], Pawel Stanczak[1], Aaron A. Thompson[1], Yingzhuo G. Yan[3], Jasmine Chen[3], Charles K. Allerston[1], Charles L. Dillard[1], Hao Xu[1], Nicholas J. Shoger[1], Jill S. Cameron[3], Mark E. Massari[3], and Kathleen Aertgeerts[1]

*Authors equally contributed to the manuscript

[1]Department of Structural Biology, Dart Neuroscience, 12278 Scripps Summit Drive, San Diego, CA 92131, USA; [2]Department of Preclinical Development, Dart Neuroscience, 12278 Scripps Summit Drive, San Diego, CA 92131, USA; [3]Department of Biology, Dart Neuroscience, 12278 Scripps Summit Drive, San Diego, CA 92131, USA

Author Email Addresses:
tho@dartneuroscience.com;jnguyen@dartneuroscience.com;jupingliu@dartneuroscience.com;pstanczak@dartneuroscience.com;Athompson@dartneuroscience.com;gyan@dartneuroscience.com;jasmine@dartneuroscience.com;callerston@dartneuroscience.com;cdillard@dartneuroscience.com;hxu@dartneuroscience.com;nschoger@dartneuroscience.com;jcameron@dartneuroscience.com;emassari@dartneuroscience.com;kaertgeerts@dartneuroscience.com

Correspondence: Dr. Kathleen Aertgeerts, Dart Neuroscience, 12278 Scripps Summit Drive, San Diego, CA 92131, USA. **E-mail:** kaertgeerts@dartneuroscience.com

Abstract

Recent innovative approaches to stabilize and crystallize GPCRs have resulted in an unprecedented breakthrough in GPCR crystal structures as well as application of the purified receptor protein in biophysical and biochemical ligand binding assays. However, the protein optimization process to enable these technologies is lengthy and requires iterative overexpression, solubilization, purification and functional analysis of tens to hundreds of protein variants. Here, we report a new and versatile method to screen in parallel hundreds of GPCR variants in HEK293 produced virus-like particles (VLPs) for protein yield, stability, functionality and ligand binding. This approach reduces the time and resources during GPCR construct optimization by eliminating lengthy protein solubilization and purification steps and by its adaptability to many binding assay formats (label or label-free detection). We exemplified the robustness of our VLP method by screening 210 GALR3-VLP variants in a radiometric agonist-based binding assay and a subset of 88 variants in a label-free antagonist-based assay. The resulting GALR3 agonist or antagonist stabilizing variants were then further used for recombinant protein expression in transfected insect cells. The final purified protein variants were successfully immobilized on a biosensor chip and used in a surface plasmon resonance binding assay.

Keywords: GPCR Recombinant Protein Expression, Protein Engineering, Virus-Like Particles, GPCR Protein Stabilization, Membrane Protein

Abbreviations: A2A, Adenosine A2A Receptor; **eGFP**, enhanced Green Fluorescent Protein; **ESI**, Electrospray Ionization; **GALR3**, Galanin Receptor Type 3; **GPCR,** G-Protein Coupled Receptor; **HA,** Hemagglutinin; **HEK**, Human Embryonic Kidney; **MS**, Mass Spectrometry; **SEC/LC-MS**, Size-Exclusion Chromatography/Liquid Chromatography Mass Spectroscopy; **SPR**, Surface Plasmon Resonance; **VLP,** Virus-Like Particle; **WT**, Wild-Type

Graphical Abstract

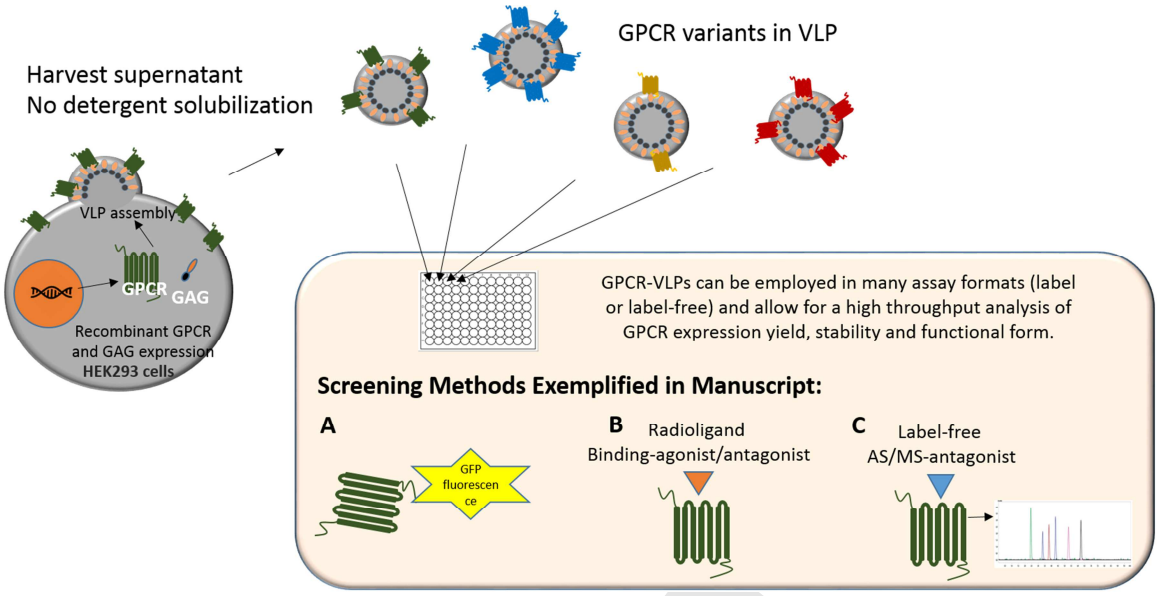

Highlights

- GPCR-VLP platform to efficiently screen for protein expression yield, stability and function.
- Versatile system that can be adopted to many assay formats (label or label-free).
- Shortens timelines for GPCR crystal structure determination and biophysical assay development.
- Expands GPCR drug discovery tools with alternative ligand screening opportunities.

1 Introduction

G-protein-coupled receptors (GPCRs) are seven-transmembrane domain receptors that mediate signal transduction initiating downstream cell signaling events triggered by a variety of small molecules, hormones, peptides and neurotransmitters. GPCRs regulate many biological processes and are linked to a wide range of disease areas [1]. As a result, the GPCR superfamily is the largest family of drug targets in the human body with an estimated 30 to 50% of marketed drugs acting directly on GPCRs or through GPCR-associated mechanisms [2]. Novel small-molecule hit identification has traditionally relied on screening ligands against GPCR overexpressing heterologous cells or homogenized cell-membrane preparations. No biophysical or biochemical assays that use purified protein material were readily available because of the lack of tools to keep GPCRs functionally intact and stable outside the cell membrane. In the past few years however, considerable progress has been made in the development of innovative approaches to express and purify these receptors in low milligram quantities [3-4].

Despite the great progress made, the process of protein engineering to overexpress and stabilize GPCRs outside of the cell membrane is tedious, costly and time-consuming. It is complicated by low protein yields and a mixed population of various conformational and functional forms of the native form of the receptor. Although this conformational flexibility is necessary for receptor coupling to multiple effectors and signaling, it hampers the formation of well-ordered crystals or the biophysical analysis of a specific functional form of the receptor. To reduce some of the structural motions, putative flexible regions have been deleted, mutations have been added and/or soluble proteins of about 15-20kDa have been fused to promote crystal contacts and stabilization [3-4]. Published processes to attain the most appropriate protein construct for biochemical, biophysical and/or structural studies can be lengthy and intricate, depending on the GPCR, and typically

includes iterative recombinant overexpression, purification and analysis of detergent-solubilized protein variants [3-4].

Here, we propose a new technology platform to express and characterize GPCRs constituted *in situ* in VLPs produced from HEK293 cell cultures. VLPs are multiprotein nanostructures assembled from viral structural proteins and contain a cellular lipid bilayer necessary to maintain the structural integrity of a GPCR. VLPs containing membrane or non-membrane proteins have been used for diverse applications in vaccination, targeted drug delivery, gene therapy and immune therapy [5]. The chemically stabilizing environment of the phospholipid bilayer in a VLP has also enabled *in vitro* biophysical assay development for GPCRs such as surface plasmon resonance to study antibody binding (6-7), confocal fluorescence microscopy for high-throughput ligand screening (8) and NMR to study ligand interactions with viral membrane proteins (9). In addition, GPCR-VLPs aided in the selection of stabilizing mutants for the agonist-bound free-fatty acid receptor 1 using a label-free binding assay [10]. In our study, we demonstrate that GPCRs in VLPs are properly folded, functionally active and can be used to study receptor protein behavior through a wide array of biochemical and biophysical technologies without the need for time consuming protein purification or detergent-solubilization. Most importantly, we provide experimental evidence that GPCR-VLP protein characteristics are similar to detergent solubilized and/or purified protein from baculovirus mediated insect cell expression or from other homogenized membrane preparations thereby making it a useful pre-screen to predict protein quality. Selection of the most appropriate detection method to study GPCR-VLP protein characteristics or to perform a ligand binding screen will depend on particular project needs and objectives, but the potential applications are numerous. Several examples are provided herein

demonstrating the versatility of this technology and its applications in GPCR drug discovery and structural studies.

2 Materials and methods

2.1 VLP Production and Analysis

DNA Plasmid Generation-The native DNA sequence coding for the 502 amino acids of HIV-1SF2 p55Gag (GenBank accession no. K02007) was codon-optimized for mammalian cell expression (DNA 2.0, Neward, CA, USA). The resulting modified HIV-1SF2 gag encoded a p55Gag protein with three amino acid changes (Asn377Thr, Ile403Thr, and Lys405Arg); the resulting amino acid sequence conformed to the sequences for other HIV-1 subtype B Gag proteins in the HIV sequence database (Los Alamos National Laboratory (GenBank accession no. AF201927)). The gene encoding for HIV-1SF2 p55Gag was subcloned into pcDNA™ 3.3-TOPO® vector (Thermo Fisher Scientific, Waltham, MA, USA) which employs the cytomegalovirus (CMV) immediate-early enhancer/promoter resulting in the plasmid pCMV-Gag (Figure S1). The DNA sequence coding for the full-length protein of the human Galanin Receptor Type 3 (GALR3) (2-368) and flanked by a hemagglutinin (HA) signal sequence/FLAG tag at the N-terminus and a Tobacco Etch Virus (TEV)-10xHis tag at the C-terminus was codon-optimized for mammalian cell expression and subcloned into the pEF6/V5-His TOPO vector (Thermo Fisher Scientific, Waltham, MA, USA). The resulting plasmid is called pEF6-GALR3 (Figure S1). The DNA sequence encoding the Adenosine A2A receptor (A2A) was codon-optimized for mammalian cells expression (DNA 2.0, Neward, CA, USA) and subcloned into pcDNA™ 3.3-TOPO® vector (Thermo Fisher Scientific, Waltham, MA, USA). A HA signal sequence/FLAG N-terminal tag and a TEV-eGFPA206K-8xhis C-terminal tag were added and the resulting plasmid is called pCMV-A2A (Figure S1). All subsequent A2A constructs contain the same bordering sequences in

addition to the coding sequences for the A2A (with/without fusions partners) as reported in Jokoola et al., 2008 and Liu et al., 2012 [11-12]. A2A and GALR3 point mutants were generated using site-directed mutagenesis.

VLP Generation-DNA encoding T4-Lysozyme or A23–L128 of apocytochrome b562RIL (BRIL, PDB: 1M6T) were synthesized as gBlocks (IDT, San Diego, CA, USA) and inserted into A2A constructs using Gibson assembly (NEB, Waltham, MA, USA). Plasmid DNA for mammalian cell transfection was prepared using PureLink HiPure Plasmid Midiprep Kits (Thermo Fisher Scientific, Waltham, MA, USA). 15ml of a 293FT cell line (Thermo Fisher Scientific, Waltham, MA, USA) suspension culture of $2.0x10^6$ cells/ml was infected with 9ug of pEF6-GALR3 or pCMV-A2A plasmid and 3ug of pCMV-Gag plasmid using X-TremeGENE HP transfection reagent (Roche), according to manufacturer's instructions. Following transfection, supernatants were harvested 48 hours later and clarified by centrifugation at 3,000 rpm for 10min at 4°C. The supernatants were treated with MembranePro precipitation reagent (Thermo Fisher Scientific, Waltham, MA, USA) according to manufacturer's instructions. The final VLP pellets were suspended in 50ul of 1x Phosphate buffered saline (PBS), 25-30% Glycerol, 1x Protease Inhibitor (Roche). Samples were frozen at -80°C until further use.

A2A-eGFP VLP fluorescence measurement-50µl wild-type (WT) or mutant A2A-VLP were centrifuged, washed once with 1xPBS buffer and then resuspended back into 50µl 1xPBS. VLP samples were loaded onto a 96-well plate for GFP fluorescence measurement (Perkin Elmer EnVision 2104 Multilabel Reader). The same sample was recovered from each well and applied to a bicinchoninic acid assay (BCA) assay to determine the total protein concentration of the individual VLPs (Pierce™ BCA Protein Assay Kit). The expression level of A2A was calculated as GFP Relative Fluorescence Units (RFU) per ng VLP.

2.2 Radioligand Binding Assays

Materials-Porcine galanin (GWTLNSAGYLLGPHAIDNHRSFHDKYGLA-NH2) was synthesized by Abgent (WuXi AppTec). Spexin NPQ (cat# 023-81, lot# 430195) was purchased from Phoenix Pharmaceuticals. SNAP 37889 was synthesized at Dart Neuroscience, LLC. [^{125}I]-porcine galanin (cat# NEX243) was obtained from Perkin Elmer. ZM241385 (cat # 1036) was purchased from Tocris Bioscience and [^{3}H]-ZM241385 (cat# ART0884) was obtained from American Radiolabeled Chemicals.

GALR3-VLP binding assays-Competition binding assays were performed using 18µl (2.4 mg/ml stock) of GALR3-VLPs and a final concentration of 0.2nM [^{125}I]-porcine galanin in Binding Buffer (50mM Tris pH 7.5, 5mM MgCl2, 1mM EDTA, 0.1% BSA, 0.1% bacitracin). Reactions (100µl) were incubated at room temperature for 1 hour with slow shaking, then terminated by rapid filtration over glass fiber filters (UniFilter-96 GF/C Microplate, Perkin Elmer Life Sciences, Boston, MA, U.S.A.) pre-soaked in a 0.5% polyethyleneimine solution. Filters were washed six times with wash buffer (50mM Tris pH 7.5, 5mM MgCl2, 1mM EDTA) and the remaining radioactivity was counted in a Microbeta Trilux counter (Perkin Elmer Life Sciences, Boston, MA, U.S.A.) using Microscint-20 (PerkinElmer Life Sciences, Boston, MA, U.S.A.). Data was plotted and K_i values were determined using Prism software (GraphPad Software Inc., San Diego, CA, U.S.A.). Saturation binding studies were performed as described above in duplicate with increasing concentrations of [^{125}I]-porcine galanin (0.1nM-50nM). Nonspecific binding was determined in the presence of 1µM porcine galanin. K_d and B_{max} values were determined in Prism using a one-site model. Thermal stability studies were performed in single point or duplicate using 6µl of GALR3-VLP per reaction. First, VLPs were incubated for 45 min at various temperatures ranging

from 30°C to 75°C in 5°C increments. After cooling to 4°C, a final concentration of 0.3nM [^{125}I]-porcine galanin in Binding Buffer was added. Reactions (200 µl) in 96 well plate format were incubated, terminated and measured as in the competitive binding assay described above. Tm values were calculated using Prism software.

A2A-VLP binding assays-A2A mutant VLPs (10µl aliquots) or WT A2A-VLPs (45µl aliquots) were first incubated for 30 minutes at various temperatures ranging from 0°C-90°C. After cooling on ice, heat treated A2A-VLPs were diluted in assay buffer (50mM Tris HCl, pH 7.5, 10mM MgCL2, 1mM EDTA, 0.2% BSA, and 0.1 U/ml adenosine deaminase). A 1:20 dilution was used for mutant A2A-VLPs and a 1:5.33 dilution was used for WT A2A-VLPs. In a 96-well non-binding surface plate (Corning, cat# 3604), 80µl of 4nM [^{3}H] ZM241385 and 80µl of diluted VLPs were added and the reactions were incubated at room temperature for 1 hour with slow shaking. Termination of the binding reactions, filter washing and counting of the remaining radioactivity were performed as described above. Tm values were calculated using Prism (GraphPad Software Inc., San Diego, CA, U.S.A.). The same assay buffer and assay plate were used for the saturation binding assay. 80µl each of diluted A2A-VLPs (1:20 dilution for mutant A2A-VLPs or 1:4 dilution for the WT A2A-VLPs) in assay buffer and 40µl of various dilutions of [^{3}H] ZM241385 (0-30nM) were incubated with 40µl of 40µM of ZM241385 or assay buffer at room temperature for 1 hour with slow shaking. The reaction was terminated as described above. B_{max} values were determined in Prism using a one-site model.

2.3 GPCR Recombinant Protein Expression, Purification and Analysis

DNA Plasmid Generation-The WT human GALR3 cDNA was synthesized and codon-optimized by DNA2.0 and then cloned into a modified pFastbac1 vector (Thermo Fisher

Scientific, Waltham, MA, USA) containing an expression cassette and an HA signal sequence followed by a Flag tag at the N-terminus and a Tobacco Etch Virus (TEV) protease site followed by a 10xHis tag at the C-terminus. A23–L128 of apocytochrome b562RIL (BRIL, PDB: 1M6T) was inserted in-between residues 215-220 of the intracellular loop3 (ICL3) of GALR3 after deletion of residues 216-219 (GPAG). The final plasmid pFastbacGALR3 was used for additional site-directed mutagenesis to introduce the desired mutations.

Protein Expression, Purification and Analysis-High titer recombinant baculoviruses (>10^8 infective viral particles per milliliter) were generated using the Bac-to-Bac Baculovirus Expression System (Thermo Fisher Scientific, Waltham, MA, USA) and were used to infect Spodoptera Frugiperda 9 (Sf9) insect cells at a density of 2×10^6 cells/mL with high titer viral stock at a multiplicity of infection of 5. Infected cells were grown at 27°C for 48-96 h prior to being harvested, and the cell pellets were stored at -80°C. GPCR-containing insect cell membranes were disrupted by dounce homogenization of cell pellets in a hypotonic buffer containing 25mM HEPES [pH 7.5], 10mM MgCl2, 20mM KCl, and protease inhibitor cocktail (Roche). For an immediate examination of GPCR protein expression level, 2µg of each cell lysate sample (measured using Pierce™ BCA Protein Assay Kit) was analyzed by SDS-PAGE followed by western blot analysis using an anti-6xHis epitope antibody (Thermo Fisher Scientific, Waltham, MA, USA). The intensity of the protein bands corresponding to the GPCR of interest was measured by the software ImageJ (https://imagej.nih.gov). For further purification, extensive washing of the membranes was performed repeatedly by dounce homogenization and centrifugation in the same hypotonic buffer, followed by a high osmotic buffer containing 1.0M NaCl, 10mM MgCl2, 20mM KCl, and 25mM HEPES [pH 7.5]. Purified membranes were then resuspended in 500mM NaCl, 20mM KCl, 50mM HEPES [pH 7.5], and 35% (v/v) glycerol, flash-frozen with

liquid nitrogen, and stored at -80°C until further use. Purified membranes were thawed and incubated with 50 μM of ligand, 500mM NaCl, 20mM KCl, 50mM HEPES [pH 7.5], and 5%glycerol (v/v), and incubated at 4°C for 1 hour. Iodoacetamide (Sigma) was then added to the membranes at a final concentration of 1 mg/mL for another 15 min before solubilization with 0.5% DDM (w/v) (n-dodecyl-β-D-maltopyranoside; Anatrace), and 0.1% cholesteryl hemisuccinate (CHS) (w/v) (Anatrace or Sigma) and slowly mixed for 3 hours at 4°C. The non-solubilized membranes were removed by ultracentrifugation at 160,000×g for 45 min. The supernatant was supplemented with 30mM imidazole [pH 7.5], and incubated with TALON IMAC resin (Clontech) overnight at 4°C. After binding, the resin was packed in a gravity flow column and washed with 15 column volumes of wash buffer 1 (WB1: 500mM NaCl, 20mM KCl, 10mM MgCl2, 50mM HEPES [pH 7.5], 5% glycerol (v/v), 1mM ATP, 25mM imidazole, 50μM antagonist/agonist, 0.05% (w/v) DDM, 0.01% (w/v) CHS); and 5 column volumes of WB2 (same as WB1, but without ATP and MgCl2), before protein elution with elution buffer (500mM NaCl, 20mM KCl, 50mM HEPES [pH 7.5], 10% glycerol (v/v), 250mM imidazole, 50μM ligand, 0.025% (w/v) DDM, 0.005% (w/v) CHS). Purified receptor was exchanged into a buffer containing 500mM NaCl, 20mM KCl, 5% glycerol (v/v), 50mM HEPES [pH 7.5], and 50μM ligand using a PD midiTrap G-25 column (GE Healthcare). GALR3 was then supplemented with ligand to a final concentration of 100μM, and concentrated from ~0.1 mg/mL to ~40 mg/mL with a 100 kDa molecular weight cut-off Vivaspin concentrator (GE Healthcare). Receptor purity and monodispersity was followed using SDS-PAGE and analytical size-exclusion chromatography (aSEC). Thermal stability was measured by a microscale fluorescent stability screen using the thiol-specific fluorochrome N-[4-(7-diethylamino-4-methyl-3-coumarinyl)phenyl]maleimide (CPM) assay [13].

2.4 Surface Plasmon Resonance (SPR)

Materials and Reagents-NiHC SPR sensorchips (polycarboxylate hydrogel, NTA derivatized, thickness 100 nM) were purchased from Xantec (Dusseldorf, Germany). HEPES buffer, pH 7.4 with NaCl, ethylenediaminetetraacetic acid (EDTA), and Ni2+ solution were purchased from GE Healthcare. Additional buffer components included MgCl2 solution (Ambion, Waltham, Massachusetts) and DDM (Anatrace, Maurnee, OH) which was used as a non-ionic detergent. Galanin (porcine) was purchased from Tocris (Avonmouth, Bristol).

Immobilization of GALR3 Protein-The immobilization buffer consisted of 10mM HEPES, 150mM NaCl, 50uM EDTA, 5mM MgCl2, 0.1% DDM, and 1% DMSO. Prior to immobilization, new NTA NiHC sensor chips were primed with buffer 3 times. Sensor chips consisted of a polycorboxylate hydrogel matrix pre-immobilized with nitrilotriacetic acid (NTA). The His-tagged GALR3 triple mutant protein was immobilized via Ni2+/NTA chelation. Briefly, 350mM ethylenediaminetetraacetic acid (EDTA) was injected as 3 x 60sec pulses at a flow rate of 100µl/min to prime the sensor surface followed by injection of a Ni2+ solution for 180sec at 10µl/min. GALR3 sample was then injected for 240sec at 10µl/min on the active flow cell and final immobilization levels of 10,000 RU were measured. Experiments were performed on a Biacore T200 with both the sample compartment and the analysis chamber held at 10˚C.

Kinetic analysis-Activity of the GALR3 protein was evaluated by serial injection of increasing concentrations of galanin or antagonist compound over the sensor surface followed by kinetic analysis. The analyte was serially diluted to concentrations of 10, 3, 1, 0.37, and 0.12µM in buffer. 1% DMSO was run in duplicate and used as a negative control. Galanin was injected for 80sec followed by a dissociation time of 300sec to allow the

response to return to baseline without the use of a regeneration step. DNS001355175 was injected for 60sec with a 300sec dissociation time. All sensorgrams were double-referenced by subtracting responses generated across the reference surface (to correct for bulk refractive index shifts and any non-specific binding to the chip surface) and the buffer control response (to remove any system artifacts). Data was analyzed using Biacore T200 Evaluation Software, version 2.0 (GE Healthcare) using a global fit to a 1:1 kinetic binding interaction model to determine ka, kd, and K_D. Because the calculated K_D for the antagonist compound was above the highest dose tested and therefore just an estimate, no kinetic data are presented here.

2.5 Mass Spectrometry (MS)

Electrospray ionization (ESI)-Mass Spectrometry (MS) spectra were acquired on a hybrid quadrupole time-of-flight mass spectrometer (Q-ToF Ultima, Waters, Manchester, UK) equipped with an automated chip-based nanoESI system (Nanomate 100, Advion Biosciences, Ithaca, NY, USA). The mass spectrometer was tuned with desolvation parameters during their transfer from solution to the gas phase to 50 V for the cone voltage and 40 V for the first ion tunnel (RF1) voltage. Acquisition times were as short as possible in order to obtain a sufficient signal intensity (approximately 70sec). C18 column 2.1mmx50mm, 1.7µM was used in UPLC system (Waters, Ireland). Calculations and curve fittings were carried out with the software MassLynx (Waters, Manchaster, UK) and GraphPad Prism (La Jolla, USA), respectively. WT and mutated GALR3 expressed in VLP were used at the concentration of 50µg/mL in 5mM PBS buffer at pH 7.4. VLP solutions were mixed with 10µM DNS000135175 compound and incubated on ice for 1 hour. Control sample contained no VLP. After incubation on ice, samples were incubated again at 13 different temperatures for 30 min: 4, 25, 27, 29, 31, 33, 35, 37, 39, 41, 45, 50 and

55°C. Upon temperature gradient treatment, samples were placed on ice for 10 min. The excess of unbound ligand was removed by SEC based on a 96-well plate. Then samples were diluted 2 times with 90% acetonitrile/0.1% formic acid in order to dissociate the population of bound ligand from receptor and measured subsequently by ESI-MS. ΔTm between WTGALR3 and single mutant GALR3 was estimated using equations (1) and (2):

$$IMS = (\Delta I4°C - \Delta I55°C)/[1 + \exp(T - Tm)] + \Delta I55°C \quad (1)$$

$$\Delta Tm = Tm(mut) - Tm(WT) \quad (2)$$

where IMS is the integral of the chromatography peak derived from the antagonist ion in the MS spectrum, ΔI4°C and ΔI55°C are the differences between chromatography integrals of measured samples and controls at 4 and 55°C, respectively, Tm is the midpoint of the sigmoidal curve, T is the temperature (°C), Tm(mut) and Tm(WT) are the midpoints of single point mutant of GALR3 and WT, respectively.

3 Results

3.1 VLPs as GPCR vehicles

VLPs are generated by overexpression in host cells of structural viral proteins such as HIV Gag Polypeptide, which has an inherent property for self-assembly at the host cell membrane to produce a macromolecular complex released into the cell media. VLPs have recently gained popularity for their diverse applications in vaccination, targeted drug delivery, gene therapy and immune therapy [5]. However, antibody research for vaccine development with GPCRs is limited and receptor antigen embedded in VLPs has been published for chemokine receptor 5 (CCR5) through which two domains (N-terminal via a 21 amino acid peptide and a 12 amino acid domain of the extracellular domain 2) were

used as antigen [14]. In our study, we generated VLPs that co-assemble with the complete GPCR recombinantly expressed and embedded in the host cell membrane. Similar approaches by which GPCR-VLPs were generated for biophysical assay development have been described before [10]. Enrichment of GPCRs within a VLP have also been described previously through which the Gag protein and the GPCR of interest were tagged with complementary interaction sites [8]. A schematic representation of GPCR-VLP generation is shown in Figure 1. We have developed and optimized the transfection protocol including optimization of the HIV Gag Polypeptide and GPCR DNA sequences, individual promotors for the two expression plasmids, plasmid ratios, transfection reagents and cell culture conditions. A detailed description of the final optimized protocol can be found in the Materials and Methods section.

3.2 Characterization of GALR3 Ligand Specificity using a Radioligand Binding Assay

First, we assessed whether GPCR-VLPs contain correctly folded and functional protein. Therefore, radioligand binding assays were conducted on VLPs containing GALR3 and results were compared to published data generated using conventional membrane preparations. GALR3 is a Class A GPCR which binds the neuropeptide hormones galanin and spexin [15-16]. Specific and saturable binding of [^{125}I]-galanin to GALR3-VLPs could be measured in a filtration assay with an apparent K_d = 4.7nM and a B_{max} = 445.8 fmol/mg determined using a one-site model (Figure 2A). These values compared well to the previously reported K_d and B_{max} of 2.23nM and 1,530 fmol/mg, respectively [15]. A B_{max} of 445.8 fmol/mg corresponds to 15 ng of GALR3 protein able to bind [^{125}I]-galanin and present on a VLP sample produced from a 1 ml HEK293 culture. Next, competitive radioligand displacement assays were run to determine K_i values for porcine galanin, human spexin and the small molecule GALR3-selective antagonist, SNAP 37889. All three

ligands bound to GALR3-VLPs with pK_i values of 7.52 ± 0.05 for galanin (30nM), 8.30 ± 0.07 for spexin (5.0nM) and 7.97 ± 0.09 for SNAP 37889 (10.7nM) (Figure 2B). Galanin and SNAP 37889 bound to GALR3-VLPs with affinities comparable to published values (Figure 2B and Table 1) [15, 17-18]. Although affinity values for spexin were not reported, Kim et al. published GALR3 radioligand binding concentration-response curves showing that spexin has an approximate binding affinity in the nanomolar range [19], consistent with our findings summarized in Table 1.

Taken together, these data demonstrate that GALR3-VLPs exhibit pharmacology comparable to traditional membrane preparations and further suggest that the VLP technology can be used to support conventional radioligand binding assay technologies.

3.3 Stabilization of GALR3 in its Agonist Form using a Radiometric Binding Assay

Next, we generated 210 GALR3 single point mutations out of a total of 368 GALR3 residues contained in the full-length WT sequence. The objective was to study the effect of each mutation on protein expression and stabilization. All amino acids were replaced by an Ala residue, and if Ala is present in the WT sequence, the residue was mutated to a Leu. These residues were predicted to be mostly located in GALR3 transmembrane helices based on computational modeling using published GPCR crystal structures. Initial rank ordering of the GALR3-VLP mutants based on expression yield was done by a radiometric assay measuring the binding of [^{125}I]-galanin to the receptor and comparing B_{max} values of the mutants relative to the B_{max} value of WT GALR3. 23 of the 210 mutants showed B_{max} (mutant)/B_{max} (WT) values of $\geq$ 1.0 (Table 1 in Ref [20]). The contribution of these mutations to the thermal stabilization of the receptor was analyzed by the same assay after applying a temperature gradient to the samples ranging from 30°C to 75°C. All 23 mutants showed an increase in thermal stability relative to WT GALR3 with an at least

4.0°C increase observed for V116A (ΔT=6.1°C), S110A (ΔT=5.6°C), L93A (ΔT=4.7°C), A49L (ΔT=4.4°C) and W50A (ΔT=4.0°C) (Table 1 in Ref [20]).

Next, 70 GALR3 mutants were recombinantly overexpressed in baculovirus infected insect cells. A total of 19 GALR3 single point mutants and 47 mutant combinations thereof were selected from the VLP radiometric screen described above. The aim of the study was to investigate how the protein parameters observed in GPCR-VLP samples compare to purified protein obtained after detergent solubilization and affinity chromatography purification. Protein expression yields as determined by SDS-PAGE/Western blot band intensities of the single mutants followed the same rank-order as the B_{max} values measured by the radiometric assay on the corresponding VLP samples (see Figure 1 and Table 1 in Ref [20]). However, in most cases, the yields were too low to purify the receptor to > 90% purity necessary to accurately measure its thermal stability. Therefore, 47 mutant combinations were made showing that the effect of the individual mutants was additive with best protein behavior for the double mutant: S110A+V116A and the triple mutant: S110A+V116A+A236L. Figure S2A shows a snakeplot of GALR3 visualizing the location of the mutations within the GPCR sequence. The double and triple mutants showed an increase of 9°C (±0.63; n=2) and 14°C (n=1), respectively in the N-[4-(7-diethylamino-4-methyl-3-coumarinyl)phenyl]maleimide (CPM)-based thermal melting point analysis (Figure 3B), and a concomitant change from aggregated to monomeric protein when compared to WT GALR3 (Figure 3A). Monomeric purified (>90%) protein yields for the double and triple mutant were 82 µg (±12; n=2) and 112 µg (±20; n=2) per liter Sf9 expression culture. The addition of galanin stabilized the protein even further with a measured CPM melting point of 62°C (n=1), which is an increase of 30°C over the un-liganded WT form (Figure 3A). Immobilization of the triple GALR3 mutant on a SPR chip was successfully achieved and provided the opportunity to study, in a label-free format, receptor binding of galanin (Figure 3C). The average binding parameters were

measured over five experiments: k_a = 2.78 x 10^4 $M^{-1}s^{-1}$ (± 1.06 x 10^4 $M^{-1}s^{-1}$); kd = 2.21 x 10^{-2} s-1 (± 6.74 x 10^{-3} s^{-1}); K_D = 805 nM (± 122 nM).

In summary, these data demonstrate that GPCRs expressed in the VLP system provide an excellent tool to predict protein characteristics at the purified protein level. In addition, protein stability in VLPs can be performed reliably even when protein yields are low.

3.4 Stabilization of GALR3 in its Antagonist Form using SEC/LC-MS, a Label-Free Assay

We used the results from the GALR3-VLP [^{125}I]-galanin binding assay to select 88 single point mutants with B_{max} values ≥80% of WT GALR3 assuming that these displayed enough receptor density to be further evaluated in a size-exclusion chromatography/liquid chromatography mass spectroscopy (SEC/LC-MS) based binding assay. Prior to SEC/LC-MS, the GALR3-VLP samples were incubated with GALR3 antagonist, DNS000135175 (K_i = 55nM) and subjected to a temperature gradient ranging from 15°C to 55°C. Before the acquisition of the LC-MS spectra of the ligand, unbound ligand was removed by SEC. A total of 5 mutants were found to stabilize the antagonist form of GALR3 by ≥4°C when compared to the WT form, and rank-ordered from most to least stabilizing as: A223L (ΔT=8.3°C), A218L (ΔT=7.2°C), R120A (ΔT=5.4°C), V116A (ΔT=4.6°C), E224A (ΔT=4.2°C). It is interesting to note that some mutants such as V116A and R120A contributed to the stabilization of both the agonist and antagonist forms of the receptor. Other mutants such as A223L, A218L and E224A selectively stabilized only the antagonist form.

These experiments were followed by expression of the individual GALR3 mutants and combinations thereof in the baculovirus/Sf9 system. As was seen with the single agonist mutants, the expression yields of the single antagonist mutants were too low to purify the receptor to > 90% purity and reliably measure its thermal stability. A total of 14 mutant

combinations were generated and the triple mutant V116A+R120A+A223L was found to be most stabilizing. A snakeplot visualizing the location of these mutations within the GALR3 sequence is shown in Figure S2B. The antagonist stabilizing triple mutant resulted in a 15-fold increase in expression yield and improvement from <20% to >85% monomeric protein when compared to WT GALR3 (Figure 4A). Monomeric purified protein yield (>90%) for this triple mutant was 65 µg (±4; n=2) per liter Sf9 expression culture. The final thermal melt points for the triple mutant were 35°C (n=1) in the absence and 42°C (±1.0; n=2) in the presence of the antagonist DNS001355175, an increase of 5°C and 12°C (±1.0; n=2), respectively, when compared to WT GALR3 (Figure 4B). The high protein quality of this GalR3 variant enabled antagonist binding studies by SPR (Figure 4C).

3.5 Retrospective Analysis of the Adenosine A2A Receptor Protein Yield-Stability-Structure Relationships

GPCR-VLP protein expression yield and thermal stability can be used as a systematic measure for predicting success in crystallography. It is exemplified in this particular application through a retrospective analysis on the A2A receptor, which is structurally one of the most studied GPCRs with 14 crystal structures publicly available. For all the published structures, either one or more of the following protein engineering strategies was used: insertion of a fusion partner, functionally stabilizing point mutants and the addition of agonist or antagonist ligands. From this pool of available crystal structures, we selected two structures identified by PDB codes 3EML [11] and 4EIY [12]. We generated VLP samples containing the corresponding A2A protein sequence (residues 2-315) fused to enhanced green fluorescent protein (eGFP) at the C-terminus. The final constructs are termed 3EML-VLP and 4EIY-VLP and are represented as snake plots in Figure S3. These

particular A2A structures were chosen because of the significant difference in X-ray diffraction resolution of 2.6Å for 3EML versus 1.8Å for 4EIY. This is likely a consequence of the choice of fusion partner in the third intracellular loop which is T4-Lysozyme in 3EML versus apocytochrome b562RIL (BRIL) in 4EIY. We also included an A2AWT-VLP sample containing the full-length native sequence of the receptor which is used as a reference and for which no crystal structure exists.

In our system, constructs showed a >7-fold and >10-fold increase in receptor concentration for 3EML-VLP and 4EIY-VLP, respectively, when compared to A2AWT-VLP as measured by eGFP fluorescence (Figure 5A). Receptor concentration was also measured by saturation binding of [^{3}H] ZM241385 and gave a similar rank order in expression yield for the individual VLP samples (Figure 5A). B_{max} values of 14.97±0.02fmol/mg, 407.7±4.4fmol/mg and 608.7±6.2fmol/mg were measured for A2AWT-VLP, 3EML-VLP and 4EIY-VLP respectively corresponding to 11ng, 113ng and 169ng of the respective A2A proteins able to bind [^{3}H] ZM241385 and present on a VLP sample produced from a 1 ml HEK293 culture. 4EIY-VLP showed an increase of 5.9°C in thermal melting point compared to 3EML-VLP (Figure 5B). As mentioned previously, increased thermal stability augments the likelihood to form well-ordered crystals, and this is reflected in the higher diffraction resolution of 4EIY-VLP when compared to 3EML-VLP. It is interesting to note that a higher thermal melt temperature was measured for A2AWT-VLP compared to 4EIY-VLP and 3EML-VLP.

4 Discussion

Over the past five years, extensive protein engineering has allowed the purification and crystallization of GPCRs in a conformationally homogeneous form which resulted in an exponential increase in the publication of new crystal structures. Complementary strategies such as amino acid truncations, fusions with readily crystallizable soluble

proteins and point mutants have proven to be the most successful [3-4]. Although these approaches are conceptually applicable to enable structural studies of other GPCRs, there is limited transferability in terms of rational construct design at the level of specific amino acid positions for truncations and insertions [3-4, 21]. Similarly, a total of about 90 thermostabilizing mutations have been identified by Alanine-scanning of various GPCRs, but the information provided limited transferability to stabilize other GPCRs for which no crystal structure exists [22]. Thus tens to hundreds of protein constructs need to be engineered to overexpress and stabilize GPCRs to facilitate biophysical assay development or structural studies. Our GPCR-VLP platform is a versatile system to examine in parallel hundreds of GPCR protein constructs and pre-screen for expression yield, specific receptor functionality and stability.

VLPs are multiprotein structures that mimic the organization and conformation of authentic native viruses but lack the viral genome. VLPs can be produced in a variety of cell culture systems including mammalian cell lines, insect cell lines, yeast, and plant cells [5]. Here, we propose to use VLPs as GPCR carriers with the following advantages: (1) in our HEK293 expression system, the VLP envelope originates from mammalian cell membranes and therefore contains the critical biochemical composition to keep GPCRs in their native and fully functional conformation; (2) VLP production is ~2 times faster than baculovirus production from Sf9 insect cells; (3) GPCRs embedded in VLPs are present under semi-purified form, removed from all other cellular organelles; (4) the concentration of VLPs can be manipulated through precipitation and resuspension; (5) VLPs can be frozen for storage without affecting receptor function (Figure S4).

In this manuscript, we demonstrate that GPCR protein quantity and quality can be pre-screened in VLPs. In contrast to previously published methods [3-4], there is no need to

solubilize or purify the individual engineered proteins to determine its amenability to structural or other biophysical studies. VLP samples contain the receptor in its ligand-unbound form and therefore can be used in diverse assay formats, each tailored to study specific functional forms of the GPCR. For example, we generated 210 GALR3 mutants in VLP and quickly assessed single data point readouts using a radiometric assay showing that 88 mutants had an improved protein yield based on receptor density (B_{max}) >80% of WT. Further delineation of these 88 mutants and their specific contribution to the stability of either the agonist or antagonist form of GALR3 was done with the same VLP samples but applying a different thermal stability assay, one using a radiolabeled agonist, the other a label-free SEC/LC-MS-based binding assay in the presence of an antagonist. Based on the high-throughput capability, sensitivity of detection, and versatility of the VLP approach, timelines and costs are cut by at least 50% in identifying a GPCR-stabilizing construct when compared to previously published methods which can entail six months of additional studies once the thermostability assays have been developed [23-24]. More recently, a new scientific report was published describing directed evolution of GPCRs in yeast. The authors describe an alternative high-throughput expression platform to efficiently optimize GPCRs for recombinant protein expression in eukaryotic expression hosts [25].

Several examples in our manuscript verified that GPCR protein characteristics in VLPs are consistent with receptor protein features after recombinant over-expression and purification. Although VLP expression is fast and efficient for small-scale studies, large-scale expression for GPCRs is challenging due to limited surface expression and high cost [26]. Recombinant over-expression systems, such as baculovirus-mediated insect cell expression, are eventually necessary to generate milligram quantities of crystallization-grade protein for structural studies and/or biophysical assay development. However, they

are expensive, time-consuming and labor-intensive and must therefore be limited to a small subset of protein constructs. For example, the GALR3 VLP Alanine scanning pre-screen of 210 single mutants resulted in the generation of 61 mutant combinations (47 for the agonist, 14 for the antagonist stabilized form) to find the best set of triple mutations that stabilized either the agonist or the antagonist form of GALR3. Importantly, these mutations changed the protein quality from a mostly aggregated WT form to a mostly monodisperse form after detergent-solubilization and purification (Figures 3A and 4A). Both forms of the receptor were successfully immobilized on a SPR chip (Figures 3C and 4C), and the antagonist GALR3 variant remained active for at least 27 hours, enabling ligand screening of large compound collections. Additionally, we show that similar substrate binding properties were measured with our GALR3-VLP samples when compared to traditionally used membrane preparations. The major advantage is that VLP samples are more consistent and homogenously prepared with less batch-to-batch variation when compared to conventional membrane samples.

A variety of detection methods can be applied to VLP samples depending on the need of the project and the availability of necessary reagents. By way of example, we used several label and label-free detection methods but the potential applications are wide-ranging. The radioligand-binding assay is considered the most sensitive detection method and can detect up to low nanogram quantities of receptor. In the absence of a radioligand, fluorescent proteins can be fused to the GPCR of interest and the fluorescent signal is then used to visualize and measure GPCR protein yield. We also demonstrate that label-free detection of thermal stability is possible by combining size-exclusion chromatography with liquid chromatography mass spectroscopy. This was particularly useful for the identification of antagonist-stabilizing mutants for our GALR3 project as no radiolabeled antagonist ligand was available at the time. A similar platform was used to find agonist-

stabilizing mutants for the free-fatty acid receptor 1 to enable its crystal structure determination [10].

In conclusion, we present a GPCR-VLP platform as a new method to efficiently assess GPCR protein characteristics including expression yield, stability, functionality and ligand binding. Our VLP technology greatly accelerates the process of GPCR construct engineering needed to enable structural studies and/or biophysical assay development. The major advantage of the GPCR-VLP platform over other routinely applied technologies is that the need for time-consuming, costly and labor-intensive solubilization and purification of the receptor is now eliminated. In addition, our studies reveal that both labelled and label-free detection methods can be used in VLPs to predict protein quality. Taken together, this work will facilitate GPCR structural biology and drug discovery in general. Additional obvious applications of the technology not exemplified in this manuscript are its use toward other integral membrane proteins or the use of GPCR-VLPs for immunization and antibody generation specifically directed toward a specific functional form of the GPCR of interest. The latter application combines the well-established adjuvant characteristics of VLPs with its GPCR carrier and stabilizing properties. Antibodies with therapeutic value can hereby be more easily generated or used to stabilize and crystallize GPCRs as observed in the beta-2 adrenergic receptor-G protein complex structure [27]. GPCR-VLPs have been used in the mobile phase and immobilized on an SPR chip to measure binding and kinetics toward antibodies as this results in a large change in refractive index due to high molecular mass binding [6-7]. As optical biosensor technologies become more sensitive, GPCR-VLPs could be immobilized directly on chip surfaces to study protein characteristics and molecular interactions with ligands or proteins.

Acknowledgements

The authors wish to thank Mr. Ken Johns, Dr. Tim Tully and Dr. James DeZazzo for critical review and feedback on the manuscript and Adi Ramon for molecular cloning support.

Funding

This research did not receive any specific grant from funding agencies in the public, commercial, or not-for-profit sectors.

5 References

[1] Conn, P. M., Ulloa-Aguirre, A., Ito, J., Janovick, J. A., G protein-coupled receptor trafficking in health and disease: lessons learned to prepare for therapeutic mutant rescue in vivo. *Pharmacol. Rev.* 2007, *59*, 225–250.

[2] Rask-Andersen, M., Almén, M.S., Schiöth, H.B., Trends in the exploitation of novel drug targets, *Nat. Rev. Drug Discov*. 2011, *10*, 579-590.

[3] Salon, J.A., Lodowski, D.T., Palczewski, K., The significance of G protein-coupled receptor crystallography for drug discovery. *Pharmacol Rev.* 2011, *63(4),* 901-937.

[4] Ghosh, E., Kumari, P., Jaiman, D., Shukla, A.K., Methodological advances: the unsung heroes of the GPCR structural revolution. *Nat Rev Mol Cell Biol.* 2015, *16(2),* 69-81.

[5] Kushnir, N., Streatfield, S.J., Yusibov, V., Virus-like particles as a highly efficient vaccine platform: diversity of targets and production systems and advances in clinical development. *Vaccine* 2012, *31(1),* 58-83.

[6] de Hoog, H.P., Lin JieRong, E.M., Banerjee, S., Décaillot, F.M., Nallani, M. Conformational antibody binding to a native, cell-free expressed GPCR in block copolymer membranes, *PLoS One.* 2014, *9(10),* e110847.

[7] Willis, S., Davidoff, C., Schilling, J., Wanless, A., Doranz, B.J., Rucker, J. Virus-like particles as quantitative probes of membrane protein interactions, *Biochemistry*. 2008, *47(27)*, 6988-6990.

[8] Heilker, R., Zemanova, L., Valler, M.J., Nienhaus, G.U. Confocal fluorescence microscopy for high-throughput screening of G-protein coupled receptors, *Curr Med Chem.* 2005;*12(22)*, 2551-2559.

[9] Antanasijevic, A., Kingsley, C., Basu, A., Bowlin, T.L., Rong, L., Caffrey, M. Application of virus-like particles (VLP) to NMR characterization of viral membrane protein interactions, *J Biomol NMR* 2016, *64(3)*,255-265.

[10] Hirozane, Y., Motoyaji, T., Maru, T., Okada, K., Tarui, N., Generating thermostabilized agonist-bound GPR40/FFAR1 using virus-like particles and a label-free binding assay. *Mol. Membr. Biol.* 2014, *31(5),* 168-175.

[11] Jaakola, V.P., Griffith, M.T., Hanson, M.A., Cherezov, V. et al., The 2.6 angstrom crystal structure of a human A2A adenosine receptor bound to an antagonist. *Science* 2008, *322(5905),* 1211-1217.

[12] Liu, W., Chun, E., Thompson, A.A., Chubukov, P. et al., Structural basis for allosteric regulation of GPCRs by sodium ions. *Science* 2012, *337(6091),* 232-236.

[13] Alexandrov, A.I., Mileni, M., Chien, E.Y., Hanson, M.A., Stevens, R.C., Microscale fluorescent thermal stability assay for membrane proteins. *Structure* 2008, *16(3),* 351-359.

[14] Hunter, Z., Smyth, H.D., Durfee, P., Chackerian, B., Induction of mucosal and systemic antibody responses against the HIV coreceptor CCR5 upon intramuscular immunization and aerosol delivery of a virus-like particle based vaccine. *Vaccine* 2009, *28(2)*, 403-414.

[15] Smith, K.E., Walker, M.W., Artymyshyn, R., Bard, J. et al., Cloned human and rat galanin GALR3 receptors. Pharmacology and activation of G-protein inwardly rectifying K+ channels. *J. Biol. Chem.* 1998, *273(36)*, 23321-23326.

[16] Mirabeau, O., Perlas, E., Severini, C., Audero, E. et al., Identification of novel peptide hormones in the human proteome by hidden Markov model screening. *Genome Res.* 2007, *17,* 320-327.

[17] Swanson, C.J., Blackburn, T.P., Zhang, X., Zheng, K. et al., Anxiolytic- and antidepressant-like profiles of the galanin-3 receptor (Gal3) antagonists SNAP 37889 and SNAP 398299. *Proc.Natl.Acad.Sci.USA* 2005, *102(48)*, 17489-17494.

[18] Konkel, M.J., Lagu, B., Boteju, L.W., Jimenez, H., et al., 3-arylimino-2-indolones are potent and selective galanin GAL3 receptor antagonists. *J. Med. Chem.* 2006, *49(13),* 3757-3758.

[19] Kim, D.K., Yun, S., Son, G.H., Hwang, J.I. et al., Coevolution of the spexin/galanin/kisspeptin family: Spexin activates galanin receptor type II and III. *Endocrinology* 2014, *155(5)*, 1864-1873.

[20] Ho, T.T., Nguyen, J.T., Liu, J., Stanczak, P., et. al., Dataset on Galanin Receptor 3 mutants that improve receptor expression and stability in an agonist and antagonist bound form. *Protein Expression and Purification Data in Brief, submitted*

[21] Chun, E., Thompson, A.A., Liu, W., Roth, C.B., et al., Fusion partner toolchest for the stabilization and crystallization of G protein-coupled receptors. *Structure* 2012, *20(6)*, 967-976.

[22] Vaidehi, N., Grisshammer, R., Tate, C.G., How Can Mutations Thermostabilize G-Protein-Coupled Receptors? *Trends Pharmacol Sci.* 2016, *37(1),* 37-46.

[23] Tate C.G. crystal clear solution for determining G-protein-coupled receptor structures *Trends Biochem Sci.* 2012, *37(9),* 343-352.

[24] Magnani, F., Serrano-Vega, M.J., Shibata, Y., Abdul-Hussein, S. et al, Mutagenesis and screening strategy to generate optimally thermostabilized membrane proteins for structural studies *Nature Protocol*s 2016, *11(8),*1554-1571.

[25] Schütz, M., Schöppe, J., Sedlák, E., Hillenbrand, M. et al., Directed evolution of G protein-coupled receptors in yeast for higher functional production in eukaryotic expression hosts. *Sci Rep.* 2016, *25*, 6:21508.

[26] Andréll J., Tate, C.G., Overexpression of membrane proteins in mammalian cells for structural studies, *Mol Membr Biol.* 2013, *30(1)*, 52-63.

[27] Rasmussen, S.G., Choi, H.J., Fung, J.J., Pardon, E. et al., Structure of a nanobody-stabilized active state of the β(2) adrenoceptor. *Nature* 2011, *469(7329),* 175-180.

Table 1. Ligand binding affinities for human GALR3

Ligand	VLP Membranes	Published Value
Porcine galanin	7.52 ± 0.05[a]	8.01 ± 0.06 [15]
human spexin	8.30 ± 0.07[a]	ND[b]
SNAP 37889	7.97 ± 0.09[a]	7.76 ± 0.01 [17]

Data are reported as pKi ± S.E.M. a) n=3. b) ND, not determined

FIGURE 1

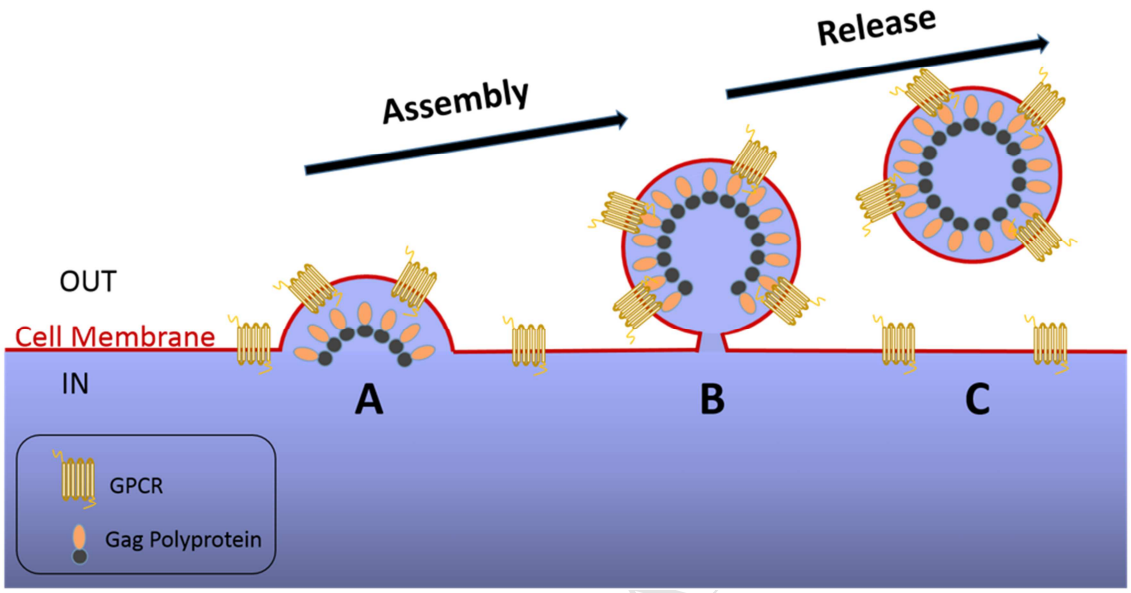

Figure 1. Schematic representation of the generation of GPCR containing Virus-Like Particles (VLPs) (A) Association of recombinantly expressed minimal HIV Gag Polypeptide proteins and GPCRs presented on the HEK293FT cell membranes. **(B)** Assembly leads to membrane fusion and pinching-off/budding of the VLP from the cell membrane. **(C)** Mature GPCR-VLPs are released in the cell culture media.

FIGURE 2

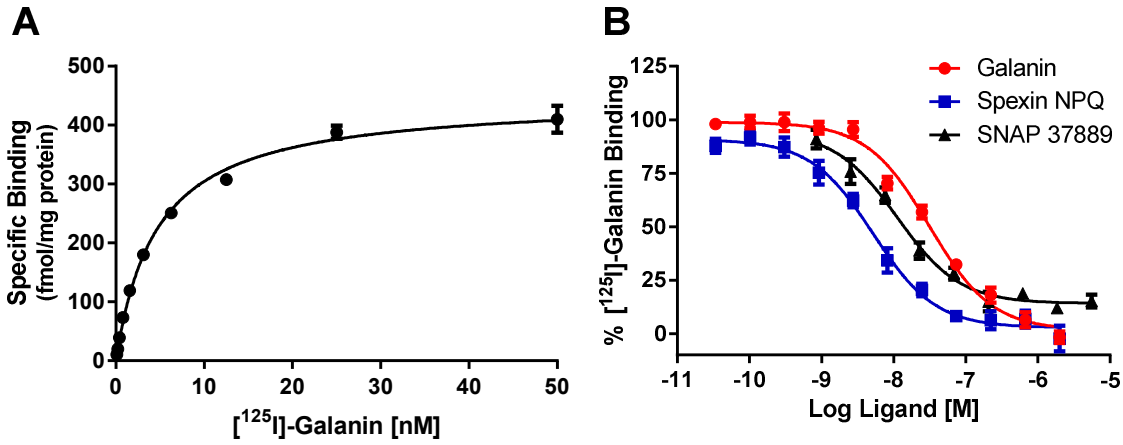

Figure 2. Radioligand binding assay with GALR3-programmed VLPs (A) Saturation isotherm for VLPs containing the WT human GALR3 receptor. Increasing concentrations of [^{125}I]-porcine galanin were incubated with GALR3-VLPs and data represent specific binding with non-specific binding values subtracted (not shown). **(B)** Radioligand binding assay concentration response curves for the GALR3 ligands galanin, spexin and the small molecule antagonist SNAP 37889. Nonspecific binding was determined in the presence of 1μM galanin. Data represent the mean ± s.e.m of three experiments, each performed in duplicate.

FIGURE 3

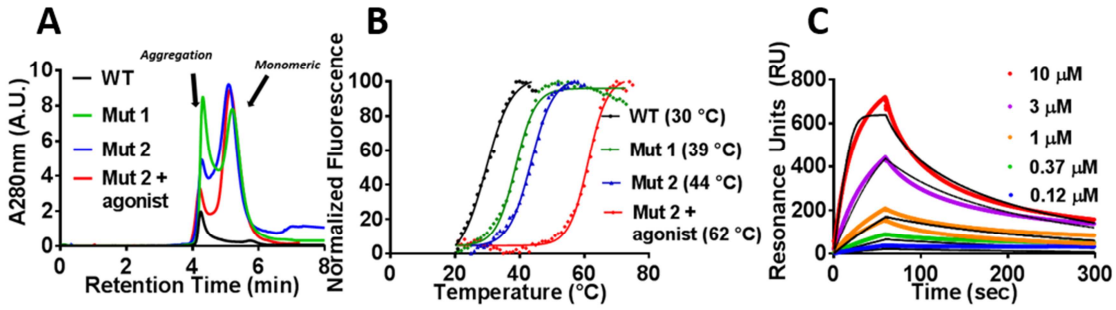

Figure 3. Protein characterization of GALR3 agonist stabilizing mutants (A) Analytical size exclusion chromatography analysis of WT GALR3, mutant 1 (Mut1: S110A+V116A) and mutant 2 (Mut2: S110A+V116A+A236L) in the absence and presence of agonist, galanin. **(B)** Thermal stability measured by the CPM assay [13] of WT and GALR3 agonist stabilizing mutants in the absence and presence of galanin. Tm values are displayed in parenthesis. **(C)** Representative raw (colored) and fitted (black) surface plasmon resonance sensorgrams of galanin binding to GALR3 Mut2. Kinetic analysis was performed using a 1:1 interaction model on the dose range shown above (replicates are included for buffer and 1μM).

FIGURE 4

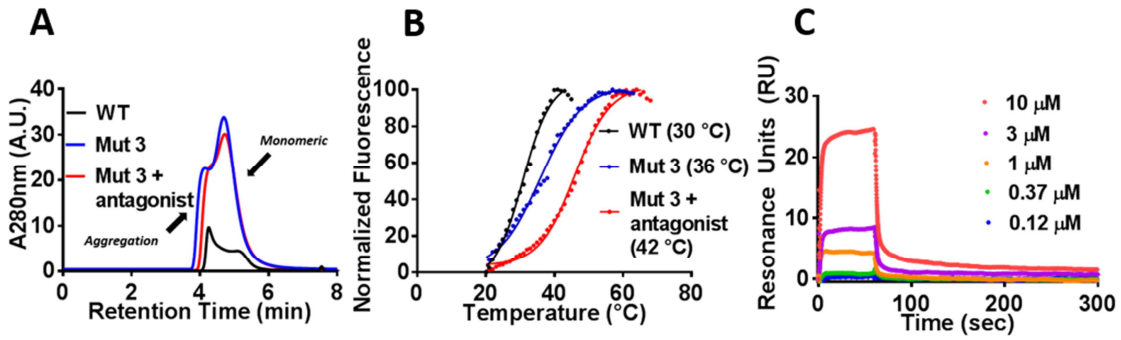

Figure 4. Protein characterization of GALR3 antagonist stabilizing mutants (A) Analytical size exclusion chromatography traces of WT GALR3 and antagonist-stabilizing mutant (Mut3: V116A, R120A, A223L) in the absence and presence of the GALR3 antagonist, DNS001355175. **(B)** Thermal stability measured by the CPM assay [13] of GALR3 WT and Mut3 in the absence and presence of the GALR3 antagonist, DNS001355175. Tm values are displayed in parenthesis. **(C)** Representative raw surface plasmon resonance sensorgrams of antagonist DNS001355175 binding to the GALR3 Mut3 (replicates are included for buffer, 0.12μM and 1μM).

FIGURE 5

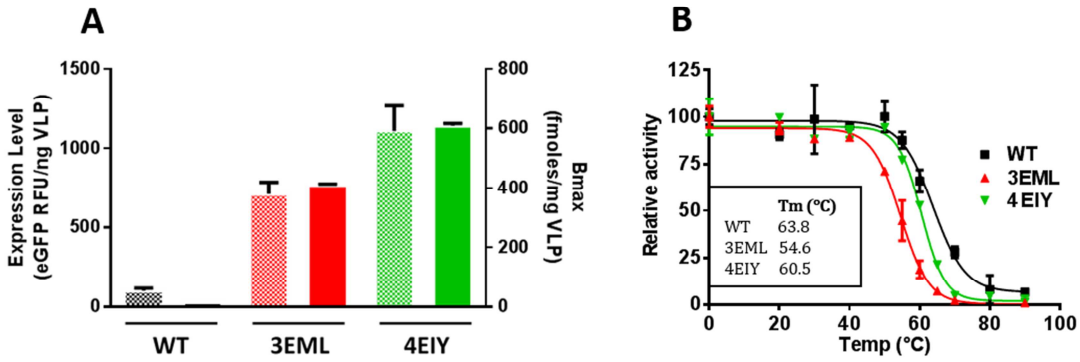

Figure 5. (A) Adenosine A2A receptor (A2A) concentration in VLP samples for different variants measured by eGFP fluorescence (dashed bars) or a radiometric binding assay using [^{3}H] ZM241385 (solid bars). Error bars are generated from three individual GFP signal measurements and two individual B_{max} calculations. WT (black) represents the full-length native sequence of A2A; 3EML (red; [11]) and 4EIY (green; [12]) are A2A variants that correspond to the protein sequences used in the crystal structures termed by the same 4 letter PDB code. **(B)** Thermal stability curves measured by a radiometric binding assay using [^{3}H] ZM241385.

Supplemental Information

Figure S1

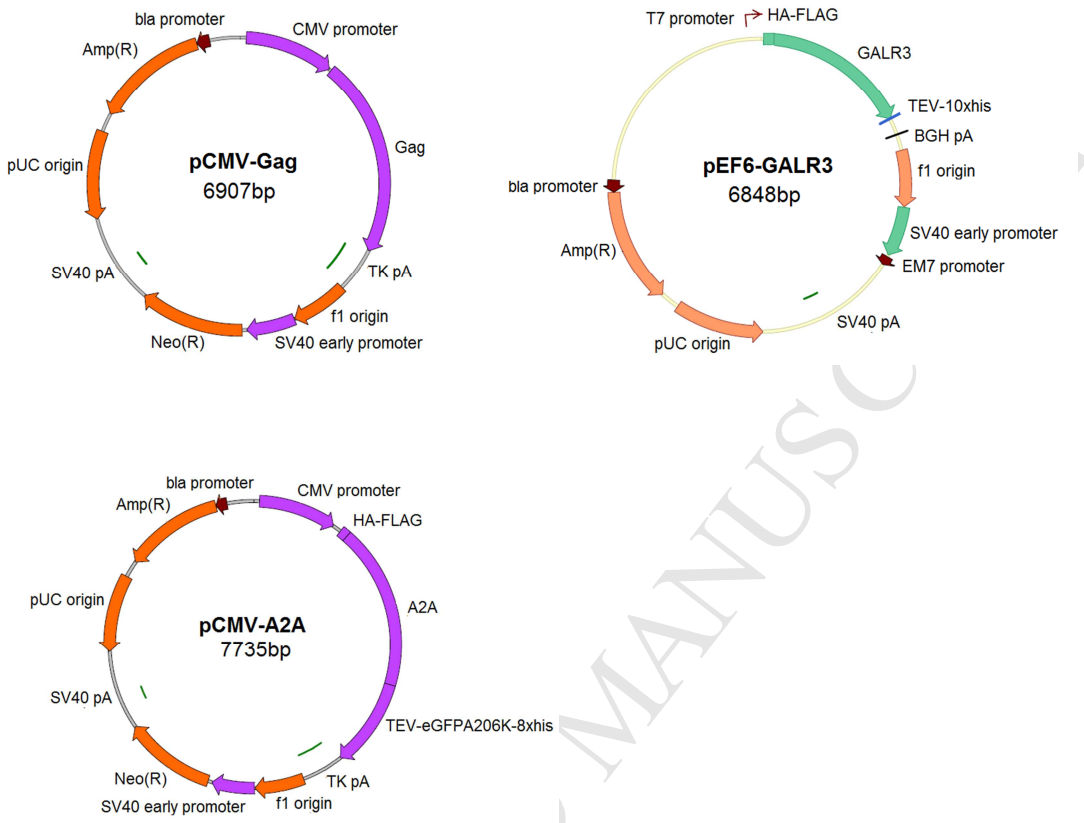

Supplemental Figure 1. Vectors used for expression of GPCRs in virus-like particles. Schematic maps of transient expression vectors (pCMV-Gag, pEF6-GALR3 and pCMV-A2A) used to produce virus-like particles containing the HIV Gag Polypeptide and GALR3 or A2A receptor protein variants.

Figure S2

A

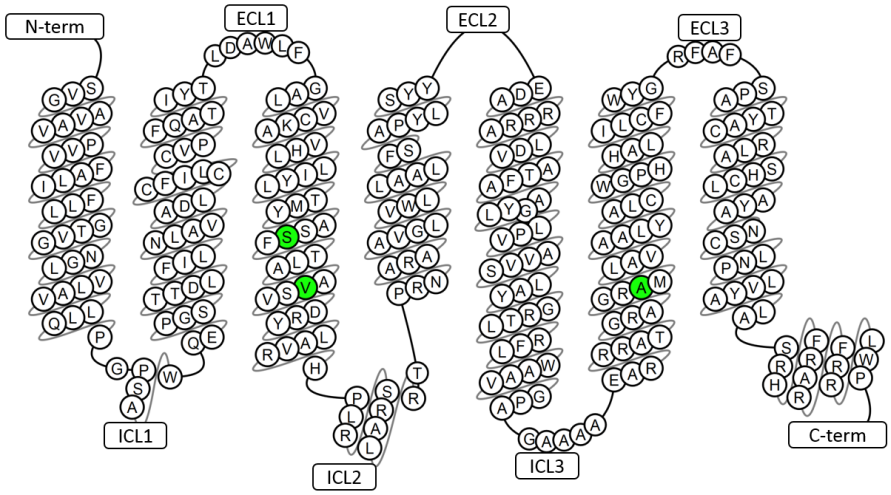

B

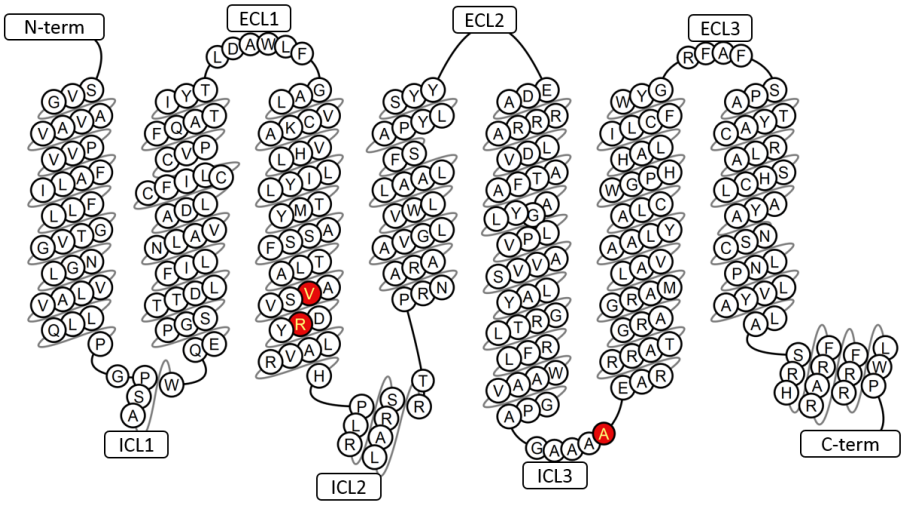

Supplemental Figure 2. Snake plots of GALR3 representing positions of (A) Agonist-stabilizing mutant and (B) Antagonist-stabilizing mutant. (A) S110, V116 and A236 are highlighted in green; (B) V116, R120 and A223 are highlighted in red. Figures were made using GPCRdb software (http://gpcrdb.org/).

Figure S3

A

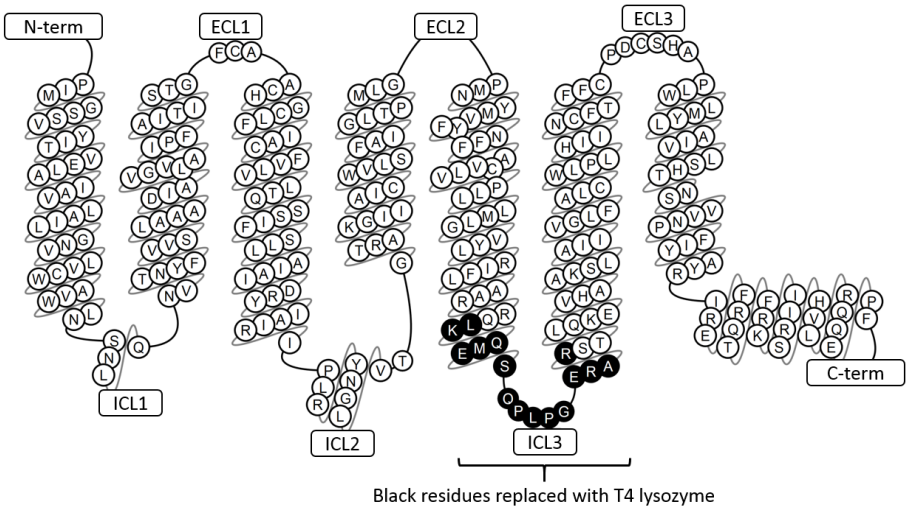

B

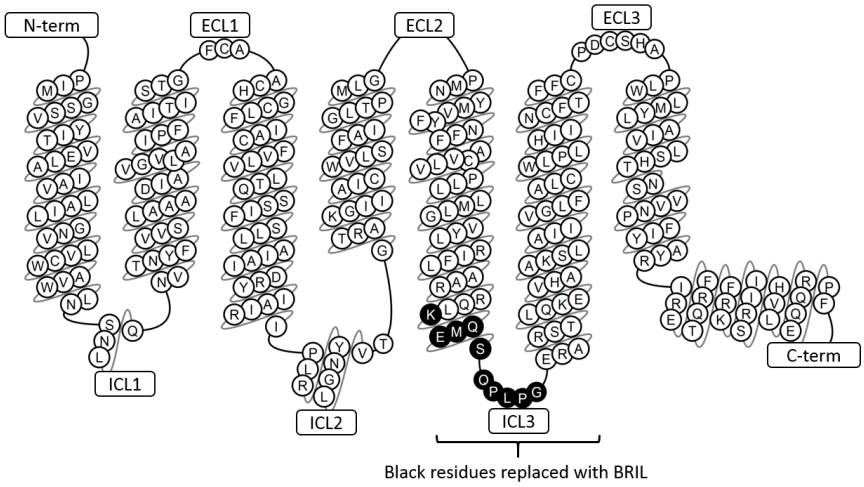

Supplemental Figure 3. Snake plots of A2A representing (A) 3EML construct and (B) 4EIY construct. Residues highlighted in black were replaced with fusion partner T4Lysozyme in 3EML and BRIL in 4EIY. Figures were made using GPCRdb software (http://gpcrdb.org/).

FIGURE S4

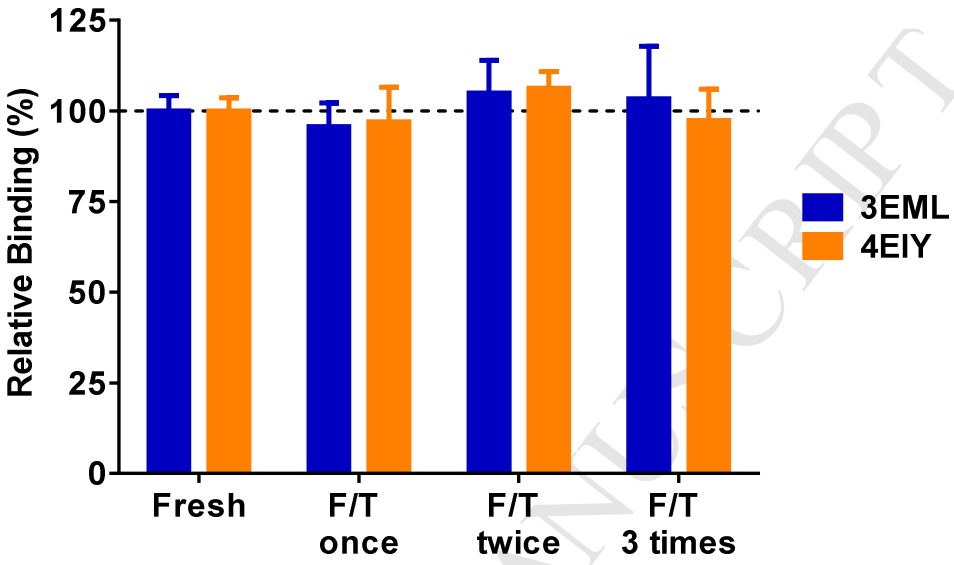

Supplemental Figure 4. Stability of A2A-VLP membranes in a radioligand binding assay. Two independent A2A-VLP mutant preparations (3EML-blue and 4EIY-orange) were tested for binding to [^{3}H]-ZM241385. VLPs (4µl/well samples, n =3) were tested fresh or subjected to 1-3 freeze-thaw (F/T) cycles prior to testing. Percent specific binding is relative to the fresh VLP sample.

Manuscript Ref: PREP_2016_230

Manuscript Title: Method for Rapid Optimization of Recombinant GPCR Protein Expression and Stability using Virus-Like Particles

Authors: Ho T. *et al.*

Highlights

- GPCR-VLP platform to efficiently screen for protein expression yield, stability and function.
- Versatile system that can be adopted to many assay formats (label or label-free).
- Shortens timelines for GPCR crystal structure determination and biophysical assay development.
- Expands GPCR drug discovery tools with alternative ligand screening opportunities.